energies

MDPI

Article

State-of-Charge Estimation for Li-Ion Power Batteries Based on a Tuning Free Observer

Xiaopeng Tang [1], Boyang Liu [1], Furong Gao [1,2,*] and Zhou Lv [2]

[1] Department of Chemical and Biomolecular Engineering, The Hong Kong University of Science and Technology, Clear Water Bay, Kowloon 999077, Hong Kong, China; xtangai@connect.ust.hk (X.T.); bliu@connect.ust.hk (B.L.)

[2] Guangzhou HKUST Fok Ying Tung Research Institute, Guangzhou 511458, China; lvzhou@ust.hk

* Correspondence: kefgao@ust.hk; Tel.: +852-2358-7139

Academic Editor: Peter J S Foot

Received: 20 July 2016; Accepted: 16 August 2016; Published: 24 August 2016

Abstract: A battery's state-of-charge (*SOC*) can be used to estimate the mileage an electric vehicle (EV) can travel. It is desirable to make such an estimation not only accurate, but also economical in computation, so that the battery management system (BMS) can be cost-effective in its implementation. Existing computationally-efficient *SOC* estimation algorithms, such as the Luenberger observer, suffer from low accuracy and require tuning of the feedback gain by trial-and-error. In this study, an algorithm named lazy-extended Kalman filter (LEKF) is proposed, to allow the Luenberger observer to learn periodically from the extended Kalman filter (EKF) and solve the problems, while maintaining computational efficiency. We demonstrated the effectiveness and high performance of LEKF by both numerical simulation and experiments under different load conditions. The results show that LEKF can have 50% less computational complexity than the conventional EKF and a near-optimal estimation error of less than 2%.

Keywords: state-of-charge (*SOC*); tuning-free; electronic vehicle; lazy-extended Kalman filter (LEKF); battery management system (BMS)

1. Introduction

Electric vehicles (EV) are a cost efficient solution to the worldwide energy crisis and environmental pollution [1]. Power sources of EVs commonly adopt lithium-based batteries, which have a high voltage, high energy density, low self-discharge rate, and long cycle life [2]. In order to improve the performance of power supply, designers sometimes integrate thousands of batteries connected in series and parallel [3], in which case, a battery management system (BMS) is required to monitor and control the working status of each single cell properly to keep the EVs safe and to extend the battery pack lifespan.

An EV BMS serves a number of functions as detailed in [4], among which the online state of charge (*SOC*) estimation for each single cell is the core one. The *SOC* of batteries is defined as the proportion of the remaining capacity to the total capacity of the battery. An accurate *SOC* estimation can not only provide the information of the remaining mileage, but also give assistance to active balancing and protection of the battery pack [5]. There are many different kinds of methods that focus on *SOC* estimation [6–22]. However, due to the limited computational ability of the embedded processor and the large amount of batteries used in EVs, the *SOC* estimation algorithm needs to be simple and reasonably accurate. Open loop approaches, such as the coulomb counting (CC) [6,7] and open circuit voltage (*OCV*) methods [8,9], are simple, but their drawbacks are significant: the CC method directly integrates the current over time to obtain the battery capacity change, leading to accumulated sensing error [23,24]. It is unlikely to provide an accurate *SOC* estimation with

an uncertain initial *SOC* value [25]. According to [4], *OCV* can reflect *SOC* in an accurate way, whereas it may take hours for the terminal voltage of a $LiFePO_4$ battery to become stable and close to the *OCV* at low temperatures. In addition to these above-mentioned specific issues, open loop approaches are also sensitive to sensor noise. Observer-based approaches are applied to solve these problems, including the Luenberger observer, proportional-integral (PI) observer, extended Kalman filter (EKF), and so on. The core theory of the observer is to estimate the *OCV* online through a battery model [26], rather than waiting for a long setting time, and then use the *OCV*-based *SOC* to correct the *SOC* obtained through the CC method. The Luenberger observer [11] is the simplest state observer, of which the logical structure is shown in Figure 1a. It uses fixed gain for state feedback, and the selection of this gain—more precisely, the pole placement of the observer system [12]—determines the convergence speed and noise filtering performance. Due to its linear property, the performance of the Luenberger observer deteriorates heavily when dealing with battery systems of strong nonlinearity [13]. The PI observer [14] provides a solution to the problem, using a proportional-integral structure to replace the constant gain. The feedback gains of these mentioned observers are mainly obtained through trial-and-error, and improper gain settings may lead to system instability. Different from the way of the PI observer, the EKF [19,20] linearizes the battery model locally and provides a minimum variance solution of Luenberger observer. It has the advantages of higher converging speed, higher accuracy, and tuning-free gain as a nonlinear adaptation. However, the cost of computation is about three times more than that of the standard Luenberger observer [27].

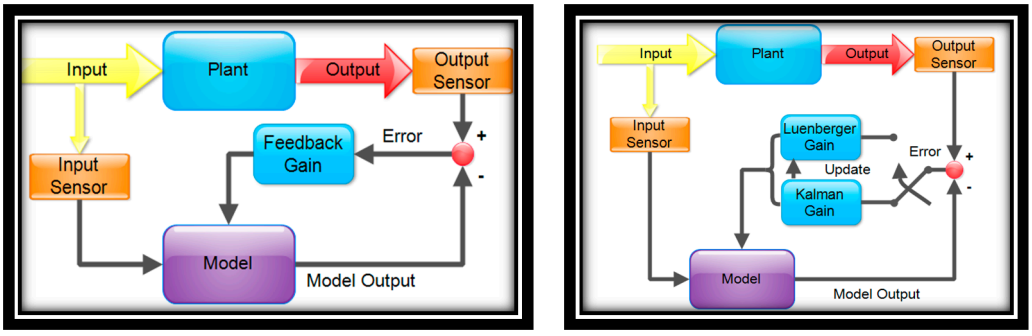

Figure 1. (**a**) General structure of the Luenberger observer and (**b**) the structure of the lazy-extended Kalman filter (LEKF).

In this paper, we introduced an idea that the inadequacy of the Luenberger observer can be compensated through learning from another optimal observer (with the same structure shown in Figure 1a). More specifically, by combining EKF with the Luenberger observer, a tuning-free observer with a structure shown in Figure 1b is established for battery *SOC* estimation. In this way, the Luenberger gain is determined online and updated intermittently with the EKF results. Noting that the intermittent EKF is less accurate than the standard EKF method [28], an updating law (Section 2.3) is proposed to ensure algorithm accuracy. The proposed algorithm can perform similarly to the standard EKF if we assume that the observing probability of intermittent EKF can be obtained. This assumption can be satisfied if a known intermitting rate strategy, for instance, in a periodical fashion, is applied. In this way, the feedback gain of the Luenberger observer can be automatically determined and, at the same time, the complexity of the proposed method can be significantly reduced while the keeping the high accuracy similar with standard EKF. The proposed method can contribute to the pack *SOC* estimation since the pack *SOC* is sometimes determined by the *SOC* of each single cell [4] and we decreased the computational cost of obtaining the single cell *SOC*. To the knowledge of the authors, this hybrid strategy has not been previously reported, and we named this method as the Lazy-Extended Kalman Filter (Lazy-EKF), as the full EKF works only occasionally. In this study, we verified the proposed method to the efficient *SOC* estimation for power battery BMS simulation.

The remainder of the paper is organized as follows: Section 2 reviews the conventional Luenberger observer and EKF algorithm, followed by the introduction of the proposed LEKF method; Section 3 displays the derivation of the LEKF method, and present numerical experiments to illustrate that the approximations and assumptions for deriving LEKF are reasonable; the performance of the LEKF method on real batteries is illustrated in Section 4 under different dynamic load conditions; and the last section reports the conclusion.

2. Lazy Extended Kalman Filter

2.1. Luenberger Observer

The definition of *SOC* is given by:

$$SOC(t) = SOC_0 + \eta \int_0^t i(\tau) d\tau / C_n \tag{1}$$

where SOC_0 is the initial state of charge, η is the coulomb efficiency, i is the current and C_n is the battery capacity. In this paper, we assume the coulomb efficiency to be 1, and use the cumulative form to replace the integral in the discrete-time cases for the following calculations. The following combined model [19] is adopted to describe a battery system:

$$V_{\text{model}} = E_0 + I_{\text{input}} \cdot r - k_0 / SOC - k_1 \cdot SOC + k_2 \cdot \ln(SOC) + k_3 \cdot \ln(1 - SOC) \tag{2}$$

where V_{model} is the model output, the terminal voltage, I_{input} is the input current, r is the battery impedance, and constants E_0, k_0, k_1, k_2, and k_3 are the battery model parameters.

The Luenberger observer is a state estimation method originally proposed by Luenberger, based on model feedback [12]. With the above stated model, the Luenberger observer can be derived to update *SOC* in the following way:

$$SOC_{k+1} = SOC_k + I_{\text{input}} / (3600 \cdot C_n) + L \cdot (V_{\text{m},k} - V_{\text{model},k}) \tag{3}$$

where C_n is the battery capacity, $V_{\text{m},k}$ is the measured voltage at time k, $V_{\text{model},k}$ is the model voltage at time k to be predicted based on Equation (2), and L is Luenberger feedback gain, the tuning parameter in the observer.

2.2. Extended Kalman Filter

The Kalman filter was first introduced to estimate battery *SOC* by Plett et al. [19,29,30] in 2004. The algorithm of extended Kalman filter can be described as follows:

For a nonlinear system:

$$\begin{cases} \mathbf{x}_{k+1} = f(\mathbf{x}_k, \mathbf{u}) + \mathbf{w}_k \\ \mathbf{y}_k = g(\mathbf{x}_k, \mathbf{u}) + \mathbf{v}_k \end{cases} \tag{4}$$

If it is linearized locally at time k:

$$\begin{cases} \mathbf{x}_{k+1} = \mathbf{A}\mathbf{x}_k + \mathbf{B}\mathbf{u} + \mathbf{w}_k \\ \mathbf{y}_k = \mathbf{C}\mathbf{x}_k + \mathbf{D}\mathbf{u} + \mathbf{v}_k \end{cases} \tag{5}$$

where $\mathbf{w}_k$ and $\mathbf{v}_k$ are independent zero-mean Gaussian noises with variance matrices $\mathbf{Q}$ and $\mathbf{R}$, respectively. Next, the process for extended Kalman filter can be described as follows:

Initialize: when $k = 0$, let:

$$\hat{\mathbf{x}}_0 = \mathrm{E}[\mathbf{x}_0] \tag{6}$$

$$\mathbf{P}_0 = [(\mathbf{x}_0 - \mathrm{E}[\mathbf{x}_0])(\mathbf{x}_0 - \mathrm{E}[\mathbf{x}_0])^{\mathbf{T}}] \tag{7}$$

Computation: for $k = 1, 2, \ldots$, compute:

$$\hat{\mathbf{x}}_k^- = f(\hat{\mathbf{x}}_{k-1}, \mathbf{u}) \tag{8}$$

$$\mathbf{P}_k^- = \mathbf{A}\mathbf{P}_{k-1}\mathbf{A}^\mathbf{T} + \mathbf{Q} \tag{9}$$

$$\mathbf{K}_k = \mathbf{P}_k^-\mathbf{C}^\mathbf{T}[\mathbf{C}\mathbf{P}_k^-\mathbf{C}^\mathbf{T} + \mathbf{R}]^{-1} \tag{10}$$

$$\hat{\mathbf{x}}_k = \hat{\mathbf{x}}_k^- + \mathbf{K}_k(\mathbf{y}_k - g(\hat{\mathbf{x}}_k^-, \mathbf{u})) \tag{11}$$

and:

$$\mathbf{P}_k = (\mathbf{I} - \mathbf{K}_k\mathbf{C})\mathbf{P}_k^- \tag{12}$$

For the battery system described in Equation (2), if we set *SOC* as the state variable, current as the input (positive when charging), and terminal voltage as output variable, we have:

$$\begin{cases} \mathbf{A} = 1 \\ \mathbf{B} = 1/(C_n \cdot 3600\ ) \\ \mathbf{C} = \frac{k_0}{x^2} - k_1 + \frac{k_2}{x} - \frac{k_3}{1-x}\Big|_{x=\hat{\mathbf{x}}_k^-} \\ \mathbf{D} = r \end{cases} \tag{13}$$

2.3. Lazy Extended Kalman Filter

In order to reducing computation cost and obtain estimation accuracy simultaneously, we constructed a hybrid strategy by using EKF to maintain its accuracy, together with the original Luenberger observer for computation efficiency. To measure the frequency of switching, we introduced an integer variable, *NC*, as the number of steps per cycle in LEKF (Figure 2). In the first step, we used EKF to estimate the *SOC*, and use the Luenberger observer in the next *NC*-1 steps in the cycle. The feedback gain for the observer is:

$$L = \frac{\mathbf{K}_n}{\sqrt{NC} + \varepsilon \cdot NC} \tag{14}$$

where K_n is the feedback gain of EKF in the n^{th} working cycle, and ε is a small number between 0 and 1. For simplicity, it was set to be 0.1 in this paper. The structure of the newly proposed method is shown in Figure 1b, where the model error is switched for the update. The working procedure of the proposed LEKF method is illustrated in Figure 2, where "update" means to use Equation (14) to obtain the Luenberger feedback gain L, and "follow" means to continue to use the previous L for the following Luenberger iteration.

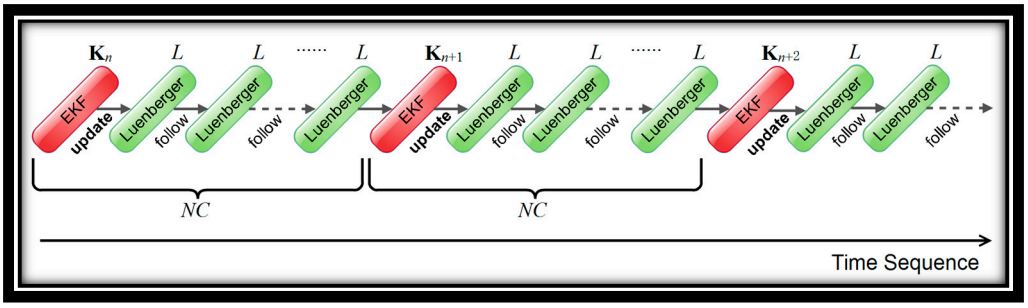

Figure 2. Procedure of the proposed LEKF method.

Based on the computation complexity defined in [27], EKF has a complexity of 16, and Luenberger observer's complexity is 5. The average complexity of LEKF can be derived as:

$$Complexity = \frac{16}{NC} + 5\frac{NC-1}{NC} \tag{15}$$

Equation (15) measures complexity in the mean sense. Clearly, the complexity of LEKF equals to that of EKF method when *NC* is set to 1. The complexity of LEKF decreases with the increase of *NC*, but the estimation error of LEKF method increases in the procedure. This is further discussed in Section 4. BMS typically runs under a real-time operating system (RTOS); therefore, it is reasonable to use mean complexity to represent computational burden in such an environment.

3. Derivation of the Lazy-Extended Kalman Filter

The key idea of the LEKF is to use Equation (14) to imitate the optimal EKF gain intermittently and reduce the computational burden. This can be done as EKF and Luenberger observers share the same structure. To simplify the derivation of Equation (14), the superscripts and the subscripts of the matrices involved are omitted.

The modified algebraic Riccati function [31] based on Equation (5) for an intermittent Kalman filter can be formulated as:

$$g_\lambda(\mathbf{X}) = \mathbf{A}\mathbf{X}\mathbf{A}^\mathbf{T} + \mathbf{Q} - \lambda\mathbf{A}\mathbf{X}\mathbf{C}^\mathbf{T}(\mathbf{C}\mathbf{X}\mathbf{C}^\mathbf{T} + \mathbf{R})^{-1}\mathbf{C}\mathbf{X}\mathbf{A}^\mathbf{T} \tag{16}$$

where λ represents the probability of the arrival of the observation, and here $\lambda = 1/NC$. In the stochastic observation problem, the arrival of the observation is usually considered as Bernoulli process with the parameter $0 < \lambda < 1$ in a wireless sensing study with packet loss [31], and the arrival of the observation is normally unknown. In this scheme, we decelerate the sampling frequency based on a known strategy to simplify the application algorithm, which is a special case of the stochastic problem.

When the Kalman filter converges, the mathematical expectation of the matrix $\mathbf{P}$ has an upper bound, which can be expressed as:

$$\mathrm{E}[\mathbf{P}] \leq \overline{\mathbf{V}} \tag{17}$$

where $\overline{\mathbf{V}}$ is the solution of the following algebraic equations:

$$\overline{\mathbf{V}} = g_\lambda(\overline{\mathbf{V}}) \tag{18}$$

for any $\mathrm{E}[\mathbf{P}_0] \geq 0$.

In Equation (13), if we treat $\mathbf{C}$ as a constant matrix, which means the system is time-invariant (this is reasonable since the *SOC-OCV* relationship can be represented in the piecewise linear form [22]), and solve Equation (18) based on Equation (13), we have:

$$g_\lambda(\overline{\mathbf{V}}) = \mathbf{A}\overline{\mathbf{V}}\mathbf{A}^\mathbf{T} + \mathbf{Q} - \lambda\mathbf{A}\overline{\mathbf{V}}\mathbf{C}^\mathbf{T}(\mathbf{C}\overline{\mathbf{V}}\mathbf{C}^\mathbf{T} + \mathbf{R})^{-1}\mathbf{C}\overline{\mathbf{V}}\mathbf{A}^\mathbf{T} \tag{19}$$

$$\lambda\mathbf{C}^2\overline{\mathbf{V}}^2 - \mathbf{Q}\overline{\mathbf{V}}\mathbf{C}^2 - \mathbf{Q}\mathbf{R} = 0 \tag{20}$$

$$\overline{\mathbf{V}} = \frac{\mathbf{Q}\mathbf{C}^2 + \sqrt{\mathbf{Q}^2\mathbf{C}^4 + 4\lambda\mathbf{C}^2\mathbf{Q}\mathbf{R}}}{2\lambda\mathbf{C}^2} \tag{21}$$

Note that the upper bound should be greater than zero.

If we further assume $\mathbf{Q}^2\mathbf{C}^4 << 4\lambda\mathbf{C}^2\mathbf{Q}\mathbf{R}$ (true for the $LiFePO_4$ battery system, since its *OCV-SOC* curve is flat when *SOC* is within 30%–80%, then $\mathbf{C}$ is close to zero, and normally $\mathbf{Q}$ is approximately equal to zero as well) then we can derive:

$$\overline{\mathbf{V}} \approx \frac{\mathbf{Q}\mathbf{C}^2 + \mathbf{C}\sqrt{\lambda\mathbf{Q}\mathbf{R}}}{\lambda\mathbf{C}^2} = NC \cdot \mathbf{Q} + \frac{\sqrt{\mathbf{Q}\mathbf{R}}}{\mathbf{C}}\sqrt{NC} \tag{22}$$

Note that in Equation (10), if assuming that $\mathbf{C}\mathbf{P}_k^- \mathbf{C}^\mathbf{T} << \mathbf{R}$ and matrix $\mathbf{P}$ is proportional to its upper bound, we obtain the following approximate relationship:

$$\mathbf{K} \propto \mathbf{P} \propto \overline{\mathbf{V}} \tag{23}$$

As previously stated, LEKF is equal to the standard EKF method when $NC = 1$, and when $NC > 1$, the intermittent Kalman filter's gain $\mathbf{K}'$ increases with NC. In Equation (22), if the following condition is true:

$$\mathbf{Q} << \sqrt{\mathbf{QR}}/\mathbf{C} \tag{24}$$

then we obtain Equation (25) to represent the relationship between the standard EKF feedback gain and the intermittent EKF feedback gain when EKF converges:

$$\mathbf{K}'/\mathbf{K} = \sqrt{NC} \tag{25}$$

where $\mathbf{K}'$ is the feedback gain of the intermittent Kalman filter with the working cycle equal to NC, and $\mathbf{K}'/\mathbf{K}$ here represents the growth multiple of the intermittent feedback gain corresponding to NC. Equation (25) can be replaced by the following equation:

$$\mathbf{K}'/\mathbf{K} = \sqrt{NC} + \varepsilon \cdot NC \tag{26}$$

Equation (26) is a good explanation of Equation (14). To illustrate the assumptions and approximations used in deriving Equation (14) are reasonable, we conducted numerical simulations of the intermittent Kalman filter to verify the proposed method.

Supposing there is a signal of which the magnitude is a constant 1, and sensing noise for measuring the signal is considerable. We applied the Kalman filter and intermittent Kalman filter (with different working periods) to estimate the magnitude of this signal. We use the mean of the feedback gain sequence to represent the general performance of the feedback gain. With the results of the intermittent Kalman filter using different working periods, we fit the relationship between the growth multiple and working periods, as shown in Figure 3.

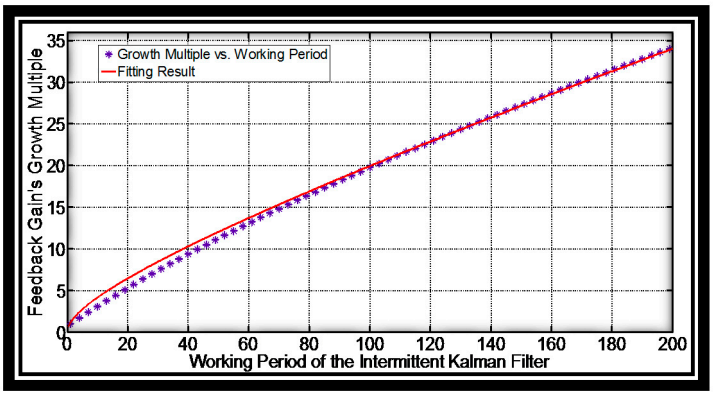

Figure 3. Relationship between the feedback gain's growth multiple and working period of the Kalman filter.

When substituting the results into Equation (26), the output least-square fitting ε is 0.09877, with the confidence interval of (0.0976, 0.09994), and the adjusted R-square of the fitting is 0.9966, which indicates the relationship in Equation (14) is reasonable and the value of ε can be chosen to be 0.1. It should be noted that the simulation is not related with the batteries, so the result should be applicable for both old and new batteries.

4. Experimental Design and Verification

In this section, we introduced the testing platform used for the experiment, followed by validation of the system model. The study is implemented under constant temperature 25 °C, the charging current is set to be positive, and the discharging current is set to be negative.

4.1. Experiment Platform

An experimental platform, as shown in Figure 4, is used with the details listed in Table 1. The analog to digital converter (ADC) in the electronic load has a resolution of 12 bits, and the controlling accuracy of the thermal chamber is ±2 °C.

(**a**) (**b**)

Figure 4. Experimental platform: (**a**) charger and discharger and (**b**) thermal chamber.

Table 1. Battery and device models.

Battery Type	Battery Capacity	Device Model
OPTIMUM 32650 Battery 1	5.00 Ah (Manufacturer Data) 5.13 Ah (Experimental Data)	Electronic Load: Sunway CT3002W Thermal Chamber: Bole GDS150

4.2. System Model Parameter Identification

As stated previously, the model of the battery is given in Equation (2). At the experimental temperature of 25 °C, the battery model parameters are identified through the least square fitting. The results are shown in Figure 5 and Table 2.

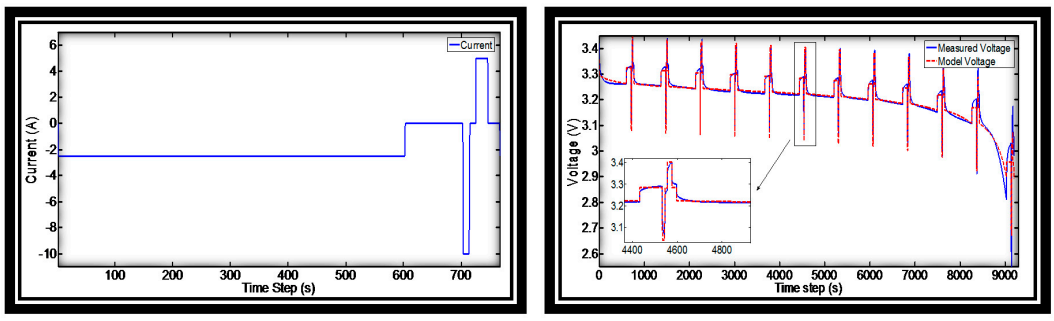

(**a**) (**b**)

Figure 5. (**a**) Load condition and (**b**) model identification result of Battery 1.

Table 2. Results of the parameter identification.

Parameter	Battery 1	Unit
E_o	3.3451	V
r	0.0242	Ω
k_0	0.0080	V
k_1	0.0500	V
k_2	0.0477	V
k_3	−0.0154	V

The *R*-square of the fitting is 0.9586, and the root mean square error (*RMSE*) is 0.0172 V. The high accuracy of the detected model parameters can support further *SOC* estimation despite that the hysteresis is not taken into account in the selected model. The differences between the measured terminal voltage and the calculated model-based terminal voltage are subtle.

4.3. Verification of the Lazy-Extended Kalman Filter Method

Here, we use loop dynamic load conditions, as shown in Figure 6a–c to verify the LEKF method on Battery 1. For comparison, we also applied the Luenberger observer and standard EKF. Since the Luenberger observer requires gain tuning, we first examined its performance with different feedback gains, and the results is best with $L = 0.01$ as shown in Figure 6d. During the entire procedure, the sampling time is set to be 1s; at the same time we have taken both current and voltage noises into consideration: standard deviation of the current noise is set to 2 A, and that of the voltage noise is set to 5 mV.

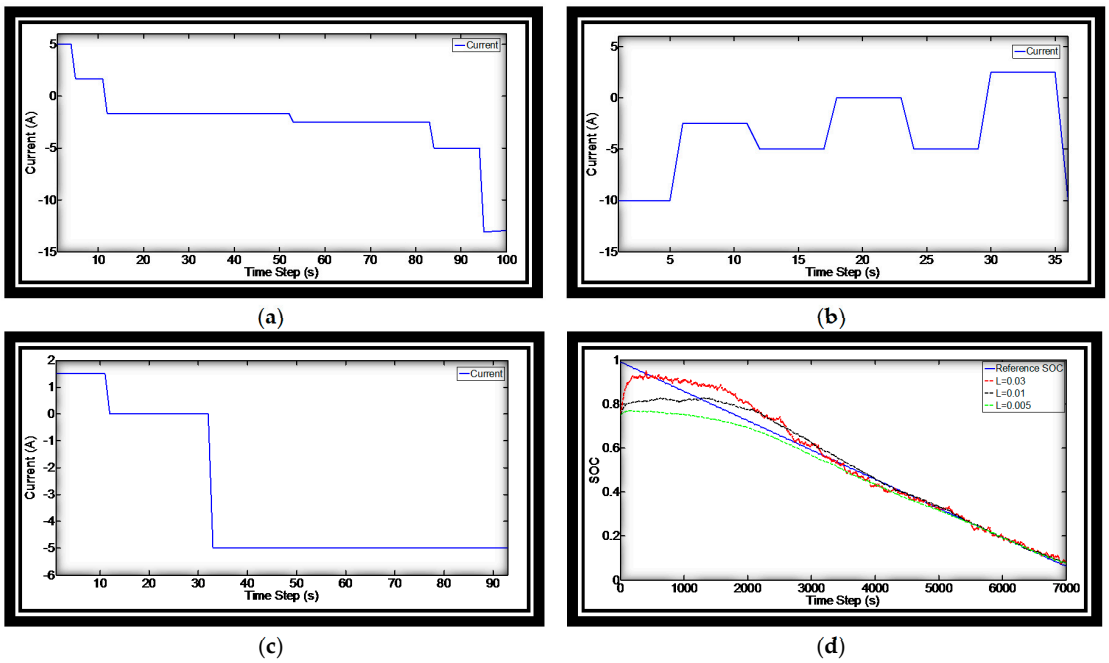

Figure 6. (**a**–**c**) dynamic load conditions; and (**d**) Luenberger observer with different feedback gains under load condition in (**a**).

Figure 7a shows compassions of the *SOC* estimation results by the Luenberger observer, EKF, and LEKF with different complexities, and Figure 7b shows the corresponding estimation errors. It can be seen that the converging speed of the LEKF is similar to that of the EKF method, which is much faster than that of the Luenberger observer. Figure 7b also demonstrates that the *SOC* estimation errors can be limited within ±2% when the complexity of LEKF is greater than 7.2, which is much better

than the national standard of many countries (e.g., mainland China, ±8%). Furthermore, the error signal of LEKF is much smoother than that of the Luenberger observer. Figure 7c shows the estimated terminal voltage of LEKF with the complexity of 7.2. It can be concluded that LEKF can estimate terminal voltage with negligible noise. Figure 7d illustrates the comparison between the measurement noise and estimation noise of the terminal voltage for LEKF with a complexity of 7.2. In general we can come to the conclusion that LEKF can generally decrease the complexity by more than 50% while maintaining accurate *SOC* estimation (with errors less than 2%).

The proposed LEKF is also evaluated with different complexities for *SOC* estimation. A plot of the *SOC* error variances against the different algorithm complexities is given in Figure 8. Generally, the decrease of complexity results in an increase in estimation error, but the relationship between them is rather nonlinear, and this nonlinear curve is lower than the linear one in the plot, which indicates the proposed LEKF can be computationally efficient with little sacrifice in accuracy.

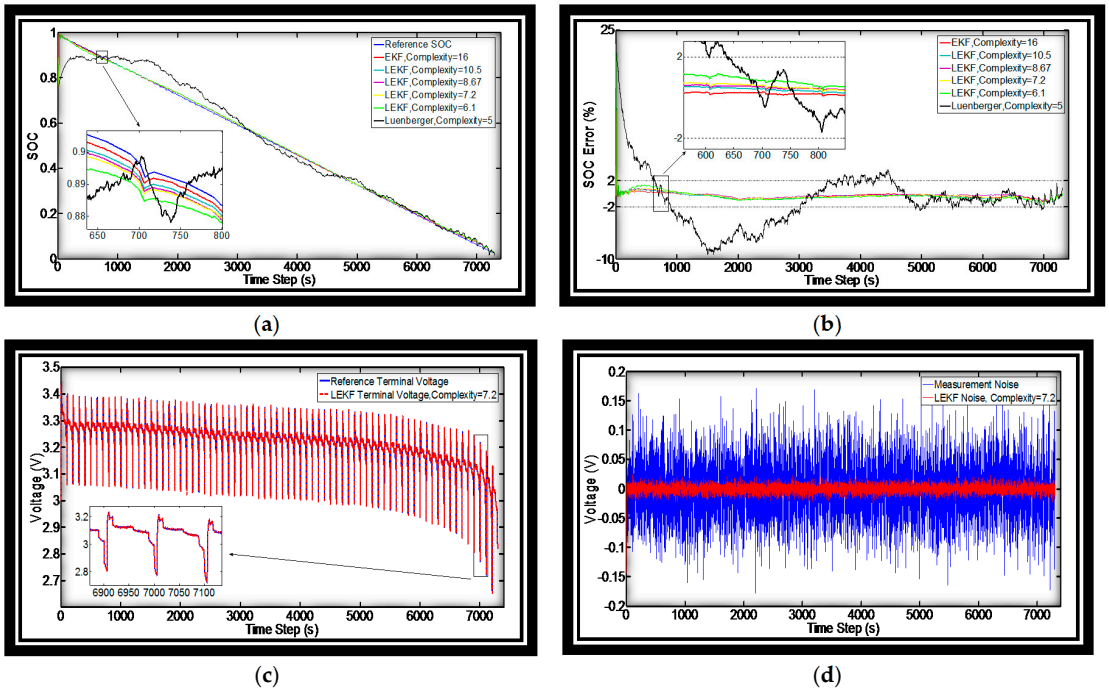

Figure 7. *SOC* estimation of different methods under load condition in Figure 6a. (**a**) *SOC* results; (**b**) *SOC* errors; (**c**) terminal voltage estimated by LEKF with complexity equal to 7.2; and (**d**) noise comparison.

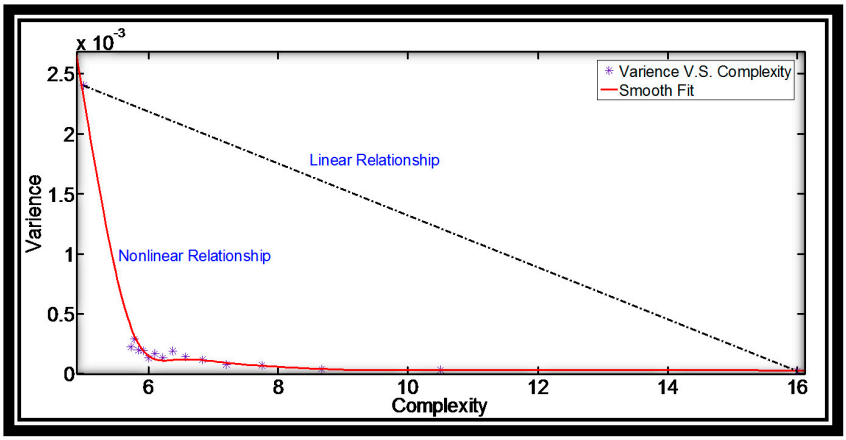

Figure 8. Relationship between variance and complexity.

The LEKF is further tested under dynamic load conditions shown in Figure 6b,c, with *NC* set to be 5 (corresponding to the LEKF complexity of 7.2). The corresponding results are shown in Figure 9. It can be seen that, in all cases, the *SOC* errors are limited within ±2% and error signals are rather smooth.

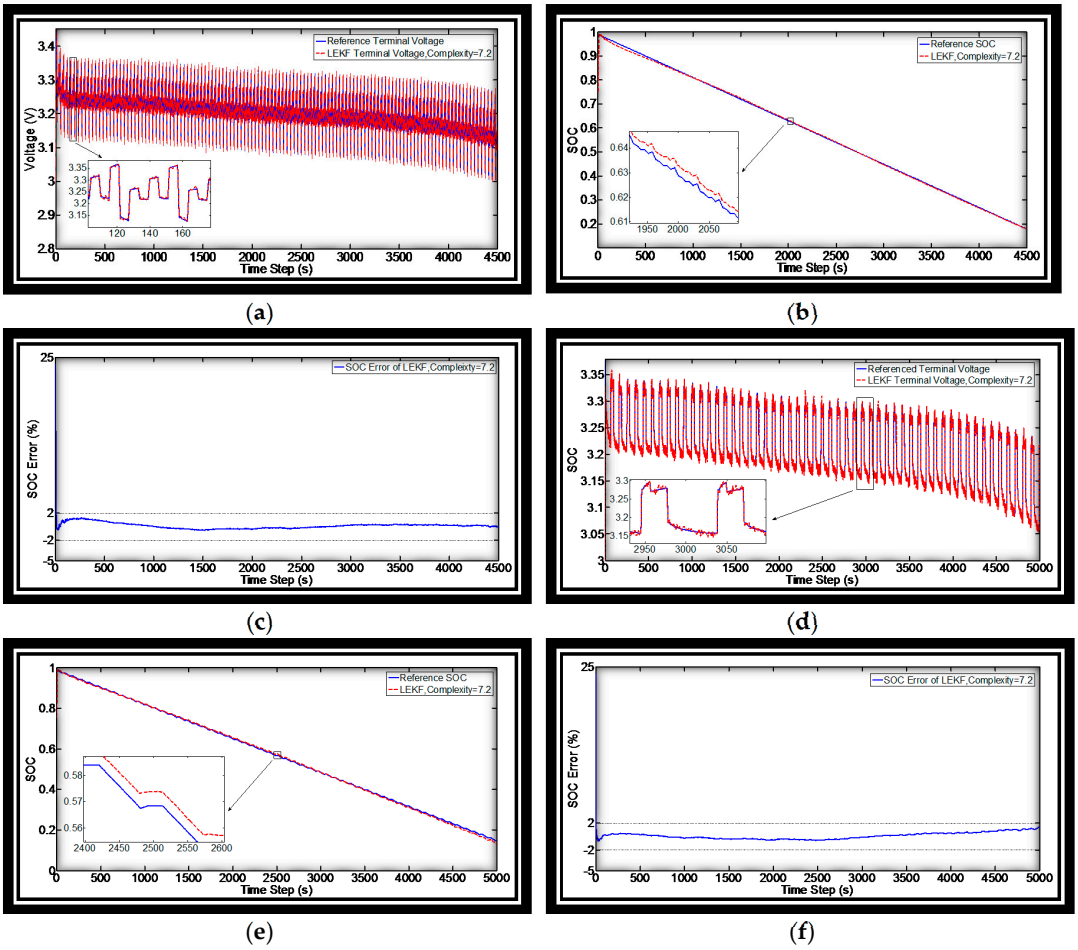

Figure 9. *SOC* estimation of different load conditions with LEKF, complexity = 7.2. (**a**–**c**): terminal voltage, *SOC*, and *SOC* error of dynamic load condition in Figure 6b; and (**d**–**f**): terminal voltage, *SOC*, and *SOC* error of dynamic load condition in Figure 6c.

We also tested the execution times and the mean absolute *SOC* estimation error of the Luenberger observer, standard EKF and LEKF of different complexities. MATLAB 2010a (MathWorks, Natick, MA, USA) was used on a laptop computer with CORE i5-5200U CPU (Samsung, Daegu, Korea), results are listed in Table 3. Only the execution times for the core codes in the iteration are counted here.

Table 3. Operating time of different algorithms.

Algorithms	Complexity (Based on Equation (15))	Operating Time	Mean Absolute *SOC* Estimation Error
EKF	16	0.166132 s	0.70%
LEKF, *NC* = 2	10.2	0.108353 s	0.75%
LEKF, *NC* = 3	8.67	0.075501 s	0.92%
LEKF, *NC* = 5	7.2	0.049359 s	1.12%
LEKF, *NC* = 10	6.1	0.040920 s	1.48%
LEKF, *NC* = 20	5.55	0.022172 s	2.52%
Luenberger	5	0.016095 s	4.67%

Despite the fact that the execution time may vary with the operating platform, programming skills, and hardware of the embedded systems, the results in Table 3 can still indicate the differences in computation costs of the algorithms. The execution time of LEKF is shorter than that of the conventional EKF in all settings, with acceptable sacrifice in accuracy. The Luenberger observer is the quickest algorithm, but its accuracy is the lowest.

5. Conclusions

A tuning-free hybrid observer, named the LEKF, has been developed and tested in this paper for *SOC* estimation of lithium-based batteries. The method uses the results of the full EKF to update the feedback gain of the Luenberger observer intermittently. LEKF has the following advantages:

(1) Lower computational complexity while maintaining the estimation with near optimal accuracy;
(2) Incorporating a tuning-free observer with no gain parameters to be tuned based on experience or by trial-and-error; and
(3) Algorithm complexity is controlled by a single variable, *NC*.

In our future work, we will focus on the battery models with consideration to the aging and temperatures of batteries. In addition, batch observation will also be investigated, understanding that cells in a pack are similar to each other.

Acknowledgments: The authors would like to thank Kaori Lkegaya and Hong Xia for helping to correct the language problems. The authors also wish to acknowledge the financial supports, in part, the Natural Science Foundation of China (NSFC) Project 61227005, and Guangzhou Science and Technology Bureau Project 2016201604030019.

Author Contributions: This research article has four authors. Xiaopeng Tang proposed the idea and wrote the paper. Boyang Liu and Zhou Lv performed the experiments and corrected the paper. Furong Gao and Zhou Lv provided the experimental resources; Furong Gao corrected the paper and made the final proof of the paper.

Conflicts of Interest: The authors declare no conflict of interest.

References

1. Lim, K.; Bastawrous, H.A.; Duong, V.-H.; See, K.W.; Zhang, P.; Dou, S.X. Fading Kalman filter-based real-time state of charge estimation in $LiFePO_4$ battery-powered electric vehicles. *Appl. Energy* **2016**, *169*, 40–48. [CrossRef]
2. Thackeray, M.M.; Wolverton, C.; Isaacs, E.D. Electrical energy storage for transportation—Approaching the limits of, and going beyond, lithium-ion batteries. *Energy Environ. Sci.* **2012**, *5*, 7854–7863. [CrossRef]
3. Etacheri, V.; Marom, R.; Elazari, R.; Salitra, G.; Aurbach, D. Challenges in the development of advanced Li-ion batteries: A review. *Energy Environ. Sci.* **2011**, *4*, 3243–3262. [CrossRef]
4. Lu, L.; Han, X.; Li, J.; Hua, J.; Ouyang, M. A review on the key issues for lithium-ion battery management in electric vehicles. *J. Power Sources* **2013**, *226*, 272–288. [CrossRef]
5. Kalawoun, J.; Biletska, K.; Suard, F.; Montaru, M. From a novel classification of the battery state of charge estimators toward a conception of an ideal one. *J. Power Sources* **2015**, *279*, 694–706. [CrossRef]
6. Ng, K.S.; Moo, C.-S.; Chen, Y.-P.; Hsieh, Y.-C. Enhanced coulomb counting method for estimating state-of-charge and state-of-health of lithium-ion batteries. *Appl. Energy* **2009**, *86*, 1506–1511. [CrossRef]
7. Yang, N.; Zhang, X.; Li, G. State of charge estimation for pulse discharge of a $LiFePO_4$ battery by a revised Ah counting. *Electrochim. Acta* **2015**, *151*, 63–71. [CrossRef]
8. Lee, S.; Kim, J.; Lee, J.; Cho, B. State-of-charge and capacity estimation of lithium-ion battery using a new open-circuit voltage versus state-of-charge. *J. Power Sources* **2008**, *185*, 1367–1373. [CrossRef]
9. Dang, X.; Yan, L.; Xu, K.; Wu, X.; Jiang, H.; Sun, H. Open-circuit voltage-based state of charge estimation of lithium-ion battery using dual neural network fusion battery model. *Electrochim. Acta* **2016**, *188*, 356–366. [CrossRef]
10. Rodrigues, S.; Munichandraiah, N.; Shukla, A. A review of state-of-charge indication of batteries by means of ac impedance measurements. *J. Power Sources* **2000**, *87*, 12–20. [CrossRef]

11. Hu, X.; Sun, F.; Zou, Y. Estimation of state of charge of a lithium-ion battery pack for electric vehicles using an adaptive Luenberger observer. *Energies* **2010**, *3*, 1586–1603. [CrossRef]
12. Luenberger, D.G. Observers for multivariable systems. *IEEE Trans. Autom. Control* **1966**, *11*, 190–197. [CrossRef]
13. Tang, X.; Wang, Y.; Chen, Z. A method for state-of-charge estimation of $LiFePO_4$ batteries based on a dual-circuit state observer. *J. Power Sources* **2015**, *296*, 23–29. [CrossRef]
14. Xu, J.; Mi, C.C.; Cao, B.; Deng, J.; Chen, Z.; Li, S. The state of charge estimation of lithium-ion batteries based on a proportional-integral observer. *IEEE Trans. Veh. Technol.* **2014**, *63*, 1614–1621.
15. Cai, C.; Du, D.; Liu, Z.; Ge, J. State-of-charge (SOC) estimation of high power Ni-MH rechargeable battery with artificial neural network. In Proceedings of the 9th International Conference on Neural Information Processing (ICONIP'02), Orchid Country Club, Singapore, 18–22 November 2002; pp. 824–828.
16. Sheng, H.; Xiao, J. Electric vehicle state of charge estimation: Nonlinear correlation and fuzzy support vector machine. *J. Power Sources* **2015**, *281*, 131–137. [CrossRef]
17. Wang, Y.; Zhang, C.; Chen, Z. A method for state-of-charge estimation of $LiFePO_4$ batteries at dynamic currents and temperatures using particle filter. *J. Power Sources* **2015**, *279*, 306–311. [CrossRef]
18. Wang, Y.; Zhang, C.; Chen, Z. On-line battery state-of-charge estimation based on an integrated estimator. *Appl. Energy* **2015**. [CrossRef]
19. Plett, G.L. Extended Kalman filtering for battery management systems of LiPB-based HEV battery packs: Part 2. Modeling and identification. *J. Power Sources* **2004**, *134*, 262–276. [CrossRef]
20. Wang, Y.; Zhang, C.; Chen, Z. A method for state-of-charge estimation of Li-ion batteries based on multi-model switching strategy. *Appl. Energy* **2015**, *137*, 427–434. [CrossRef]
21. Li, D.; Ouyang, J.; Li, H.; Wan, J. State of charge estimation for $LiMn_2O_4$ power battery based on strong tracking sigma point Kalman filter. *J. Power Sources* **2015**, *279*, 439–449. [CrossRef]
22. Dong, G.; Zhang, X.; Zhang, C.; Chen, Z. A method for state of energy estimation of lithium-ion batteries based on neural network model. *Energy* **2015**, *90*, 879–888. [CrossRef]
23. Sepasi, S.; Roose, L.R.; Matsuura, M.M. Extended Kalman filter with a fuzzy method for accurate battery pack state of charge estimation. *Energies* **2015**, *8*, 5217–5233. [CrossRef]
24. Sepasi, S.; Ghorbani, R.; Liaw, B.Y. Inline state of health estimation of lithium-ion batteries using state of charge calculation. *J. Power Sources* **2015**, *299*, 246–254. [CrossRef]
25. Sepasi, S.; Ghorbani, R.; Liaw, B.Y. A novel on-board state-of-charge estimation method for aged Li-ion batteries based on model adaptive extended Kalman filter. *J. Power Sources* **2014**, *245*, 337–344. [CrossRef]
26. Nikdel, M. Various battery models for various simulation studies and applications. *Renew. Sustain. Energy Rev.* **2014**, *32*, 477–485.
27. Barillas, J.K.; Li, J.; Günther, C.; Danzer, M.A. A comparative study and validation of state estimation algorithms for Li-ion batteries in battery management systems. *Appl. Energy* **2015**, *155*, 455–462. [CrossRef]
28. Shi, L.; Epstein, M.; Murray, R.M. Kalman filtering over a packet-dropping network: A probabilistic perspective. *IEEE Trans. Autom. Control* **2010**, *55*, 594–604. [CrossRef]
29. Plett, G.L. Extended Kalman filtering for battery management systems of LiPB-based HEV battery packs: Part 1. Background. *J. Power Sources* **2004**, *134*, 252–261. [CrossRef]
30. Plett, G.L. Extended Kalman filtering for battery management systems of LiPB-based HEV battery packs: Part 3. State and parameter estimation. *J. Power Sources* **2004**, *134*, 277–292. [CrossRef]
31. Sinopoli, B.; Schenato, L.; Franceschetti, M.; Poolla, K.; Jordan, M.; Sastry, S.S. Kalman filtering with intermittent observations. *IEEE Trans. Autom. Control* **2004**, *49*, 1453–1464. [CrossRef]